Limitation of Radiometry Model

- Surface reflection ρ can be a function of viewing and/or illumination angle

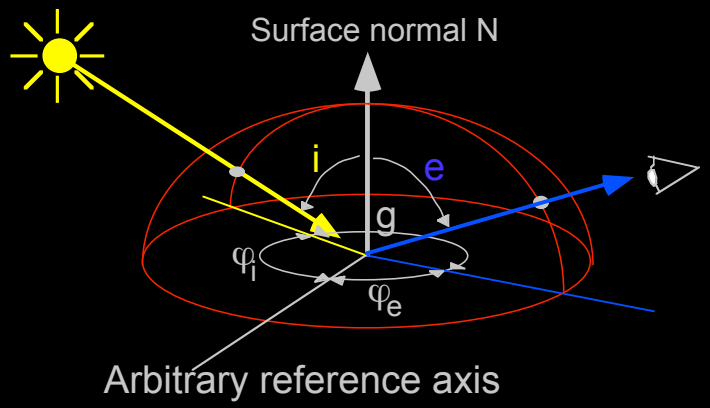

$$\rho(i,e,g,\varphi_e,\varphi_i) = \frac{dL(e,\varphi_e)}{dE(i,\varphi_i)}$$

- ρ may also be a function of the wavelength of the light source
- Assumed a point source (sky, for example, is not)

Lambertian Surfaces

- The BRDF for a Lambertian surface is a constant
  - $\rho(i,e,g,\varphi_e, \varphi_i) = k$
  - function of cos e due to the foreshortening effect
  - k is the 'albedo' of the surface
  - Good model for diffuse surfaces
- Other models combine diffuse and specular components (Phong, Torrance-Sparrow, Oren-Nayar)
- References available upon request

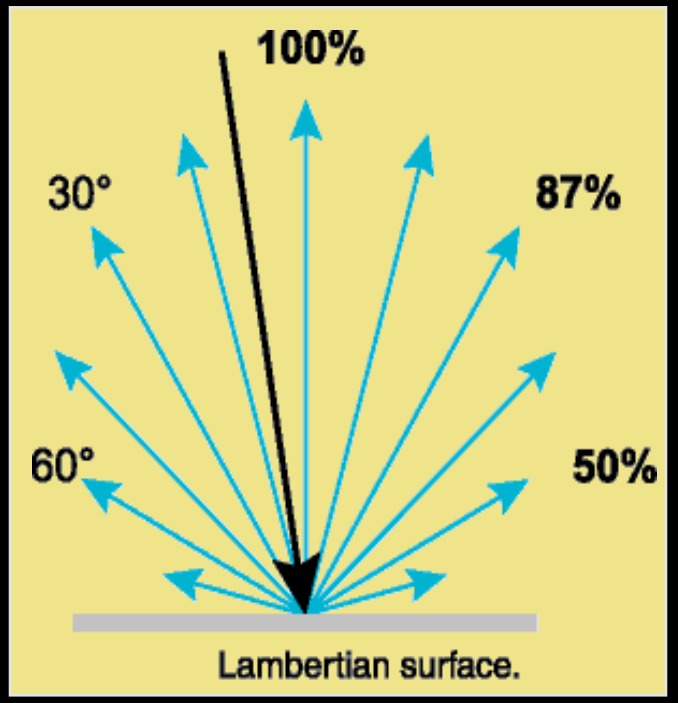

BRDF

- Ron Dror's thesis

Reflection parameters

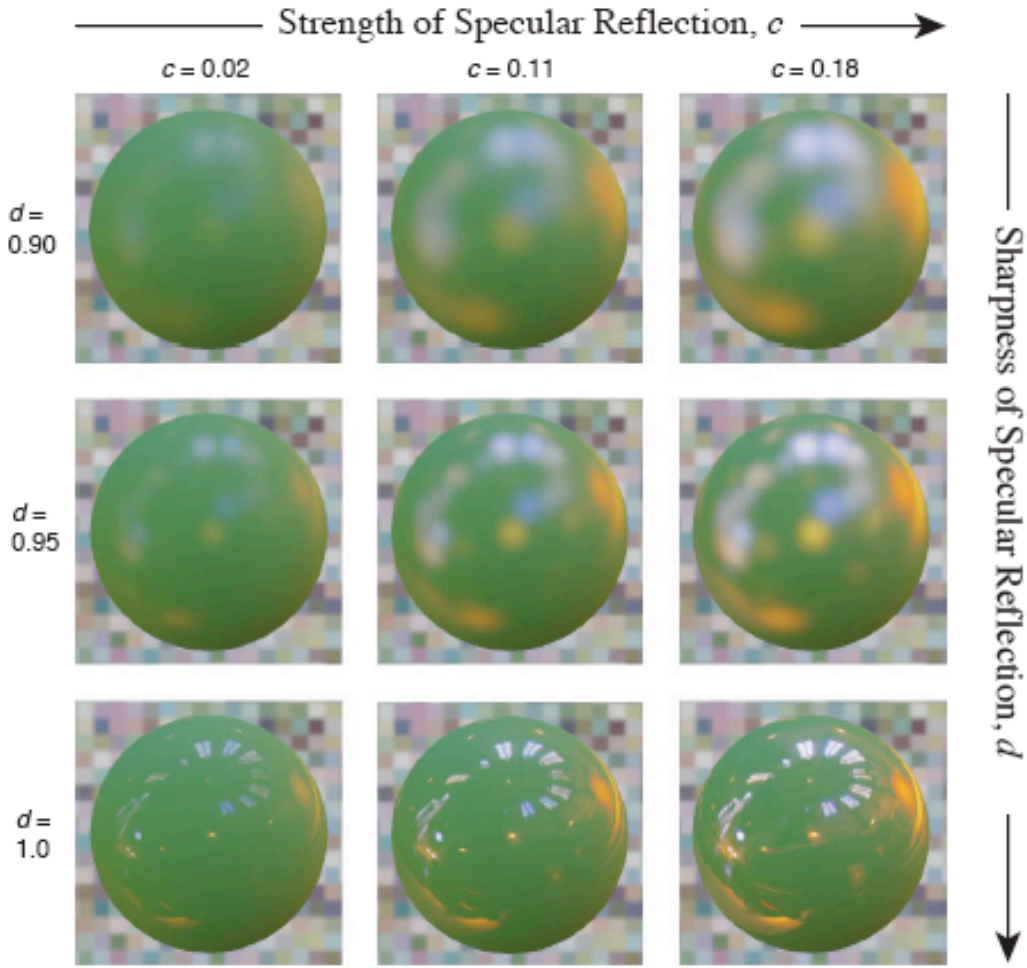

Figure 2.6. Grid showing range of reflectance properties used in the experiments for a particular real-world illumination map. All the spheres shown have an identical diffuse component. In Pellacini's reparameterization of the Ward model, the specular component depends on the c and d parameters. The strength of specular reflection, c, increases with ρ_s, while the sharpness of specular reflection, d, decreases with α. The images were rendered in *Radiance*, using the techniques described in Appendix B.

Real World Light Variation

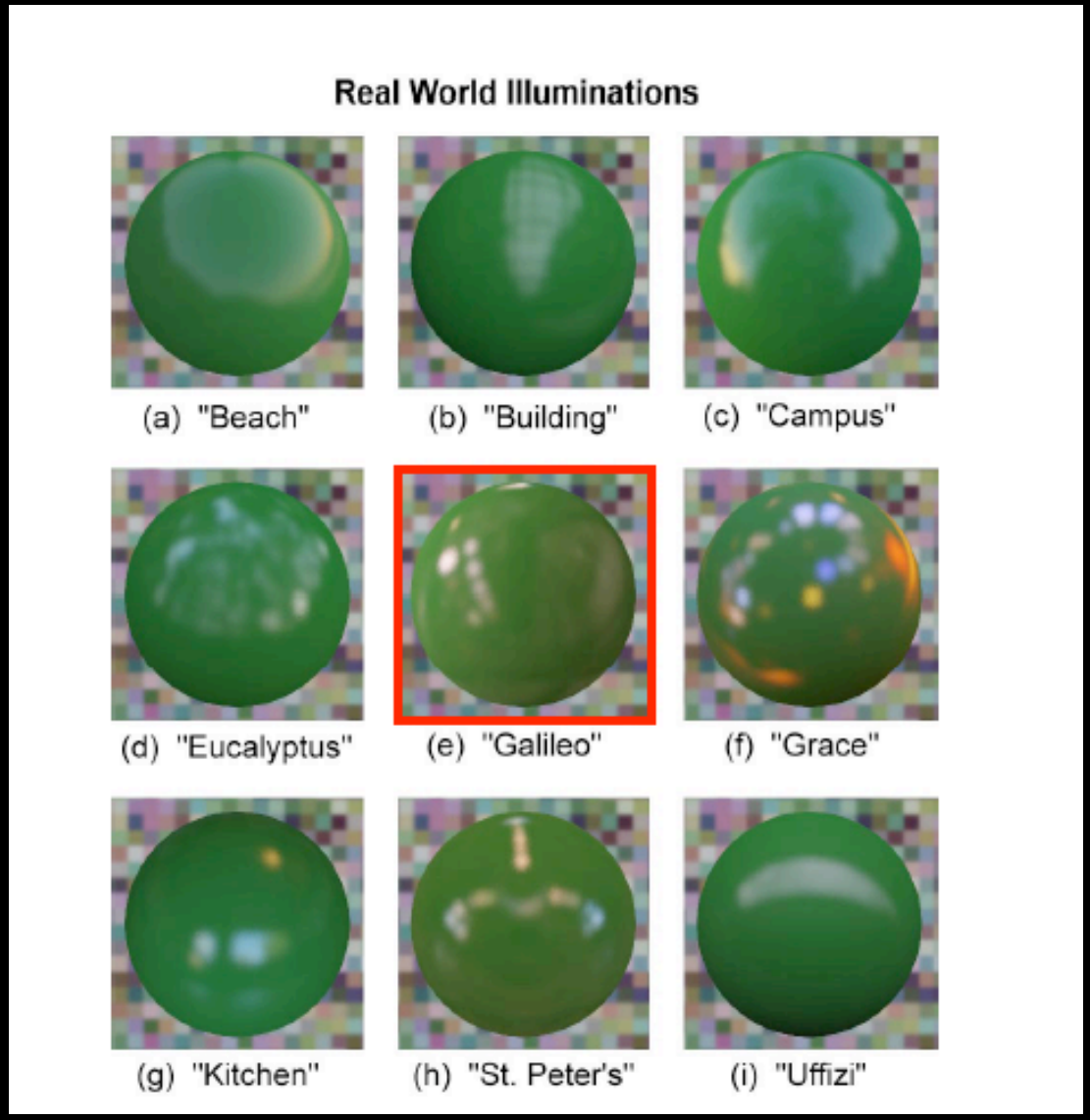

Fake Light and Real Light

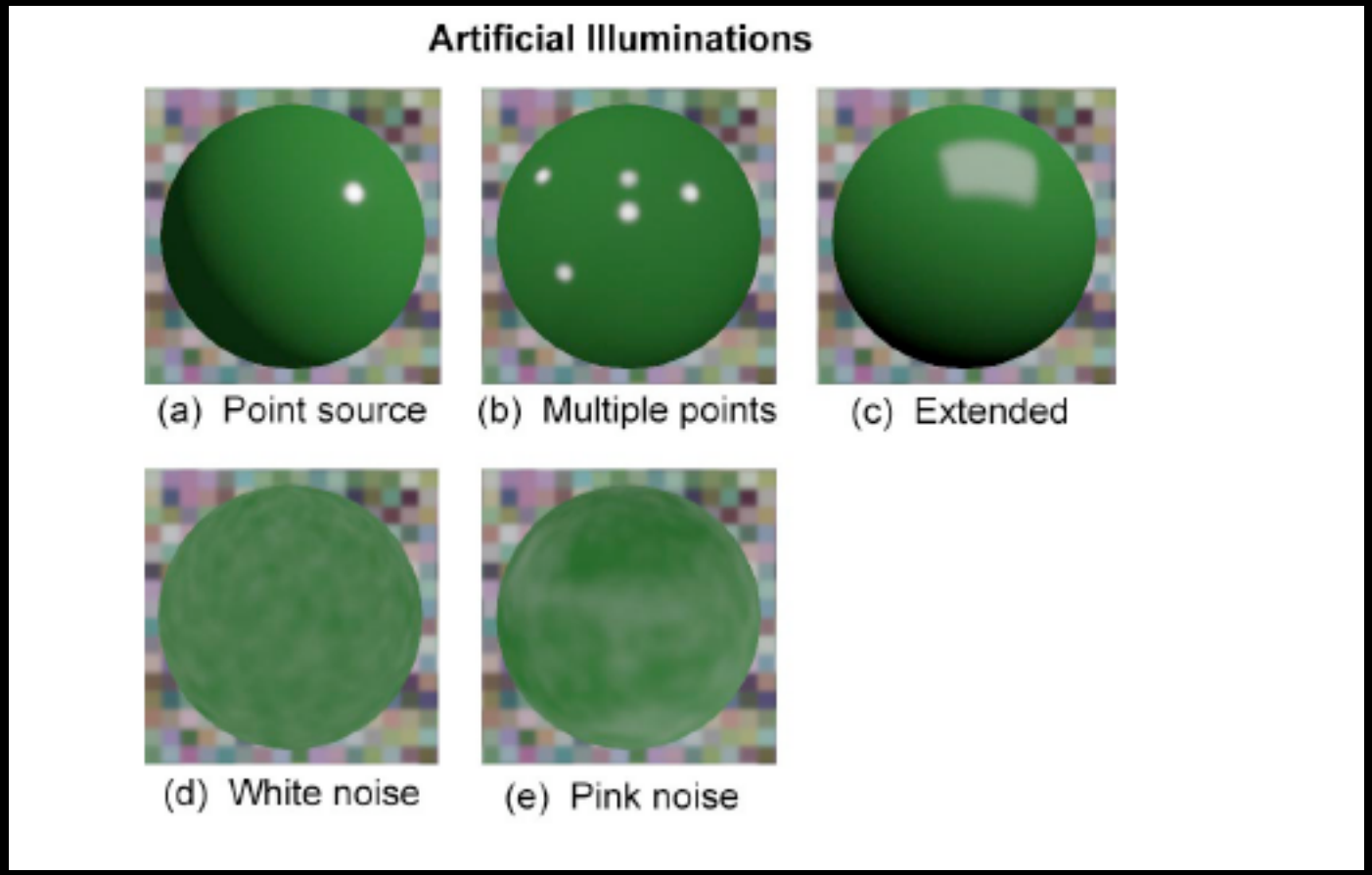

Simple and Complex Light

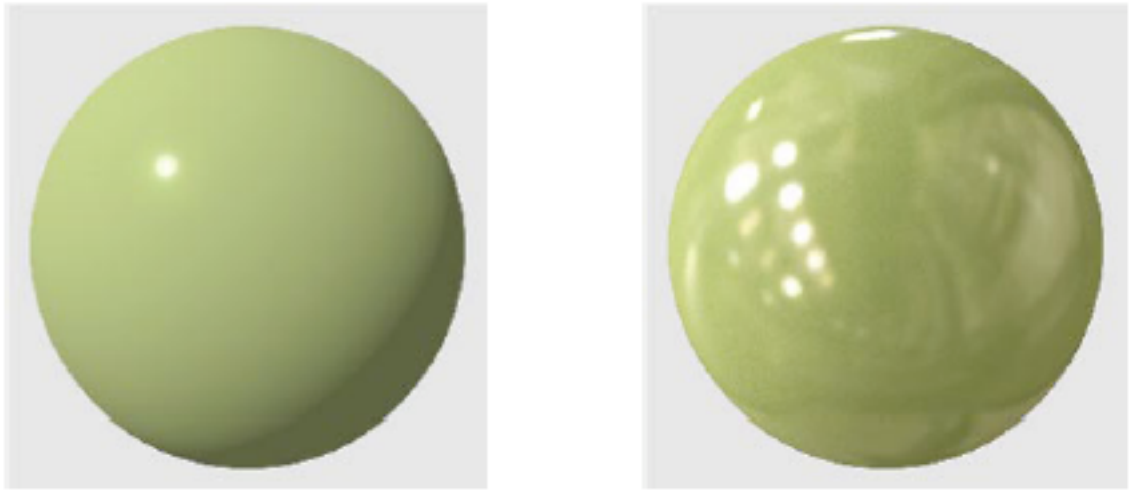

(a) (b)

Figure 2.9. (a) A shiny sphere rendered under illumination by a point light source. (b) The same sphere rendered under photographically-acquired real-world illumination. Humans perceive reflectance properties more accurately in (b).

BRDF again

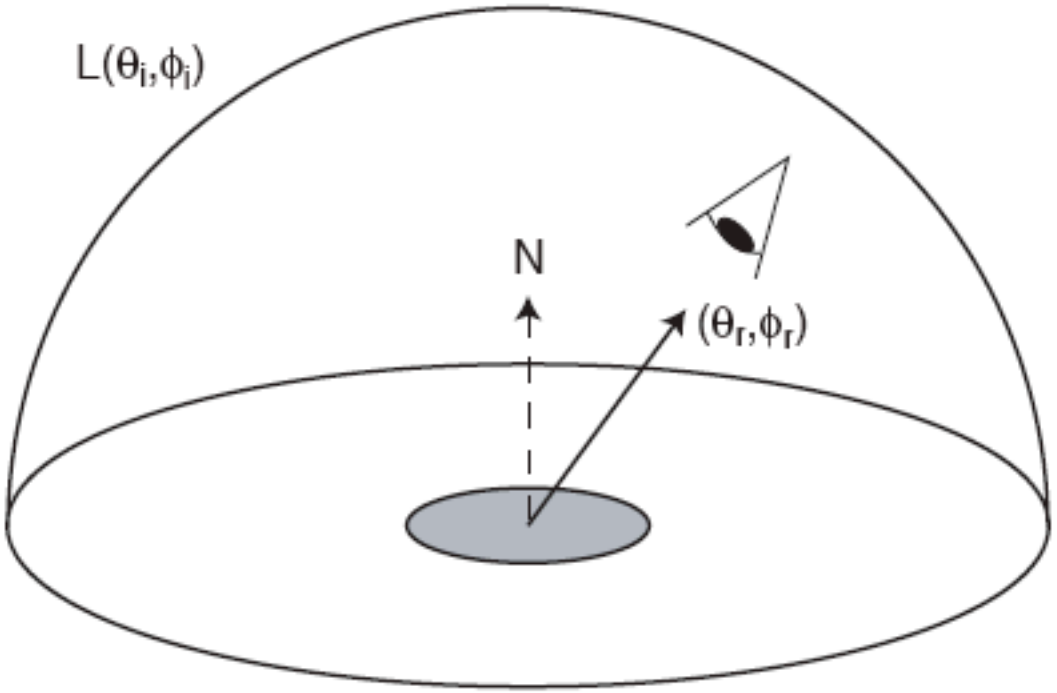

Figure 3.1. A viewer observes a surface patch with normal N from direction (θ_r, ϕ_r). $L(\theta_i, \phi_i)$ represents radiance of illumination from direction (θ_i, ϕ_i). The coordinate system is such that N points in direction $(0, 0)$.

$$B(\theta_r, \phi_r) = \int_{\phi_i=0}^{2\pi} \int_{\theta_i=0}^{\pi/2} L(\theta_i, \phi_i) f(\theta_i, \phi_i; \theta_r, \phi_r) \cos\theta_i \sin\theta_i \, d\theta_i \, d\phi_i,$$

Figure 3.6. A photograph of a matte sphere, shown against a uniform gray background. This image could also be produced by a chrome sphere under appropriate illumination, but that scenario is highly unlikely.

Classifying Under Uncertainty

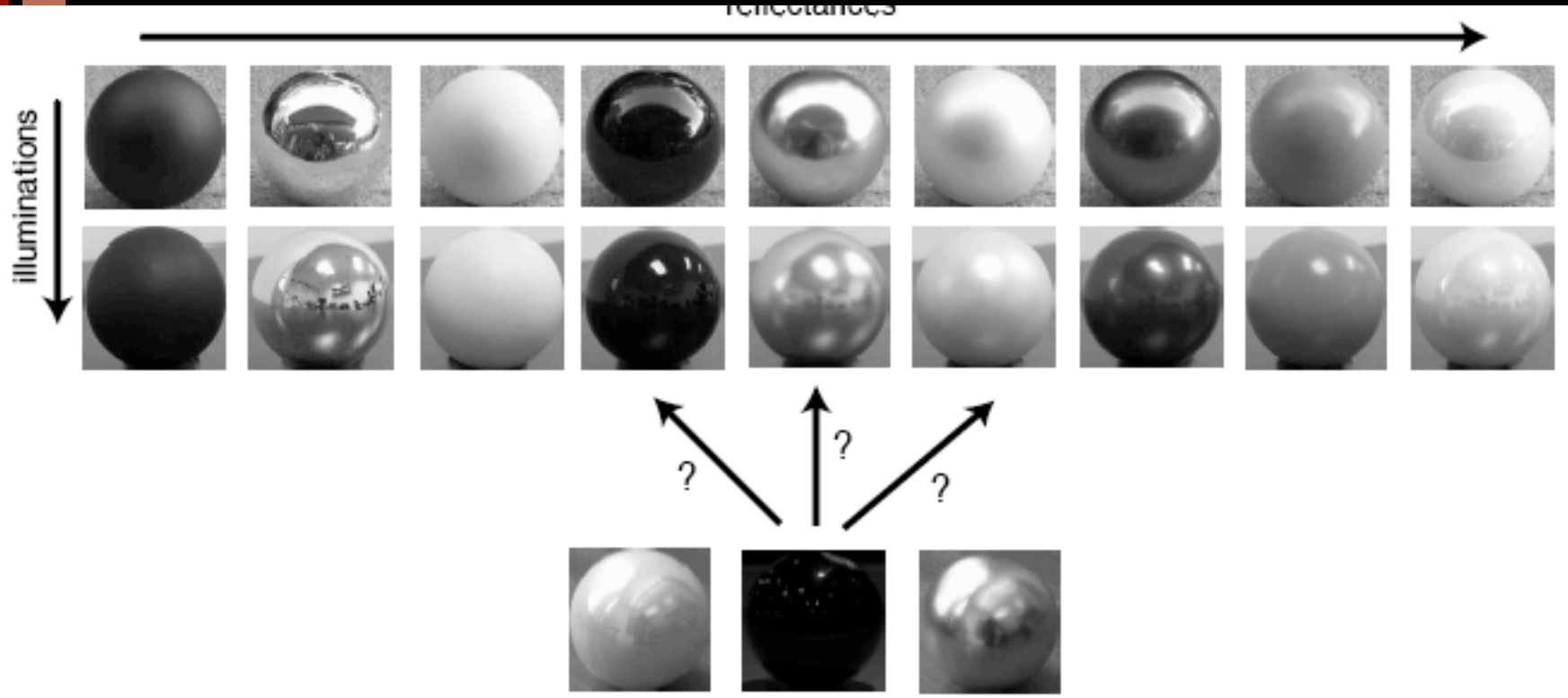

Figure 3.7. The problem addressed by a classifier of Chapter 6, illustrated using a database of photographs. Each of nine spheres was photographed under seven different illuminations. We trained a nine-way classifier using the images corresponding to several illuminations, and then used it to classify individual images under novel illuminations.

More Fake Light

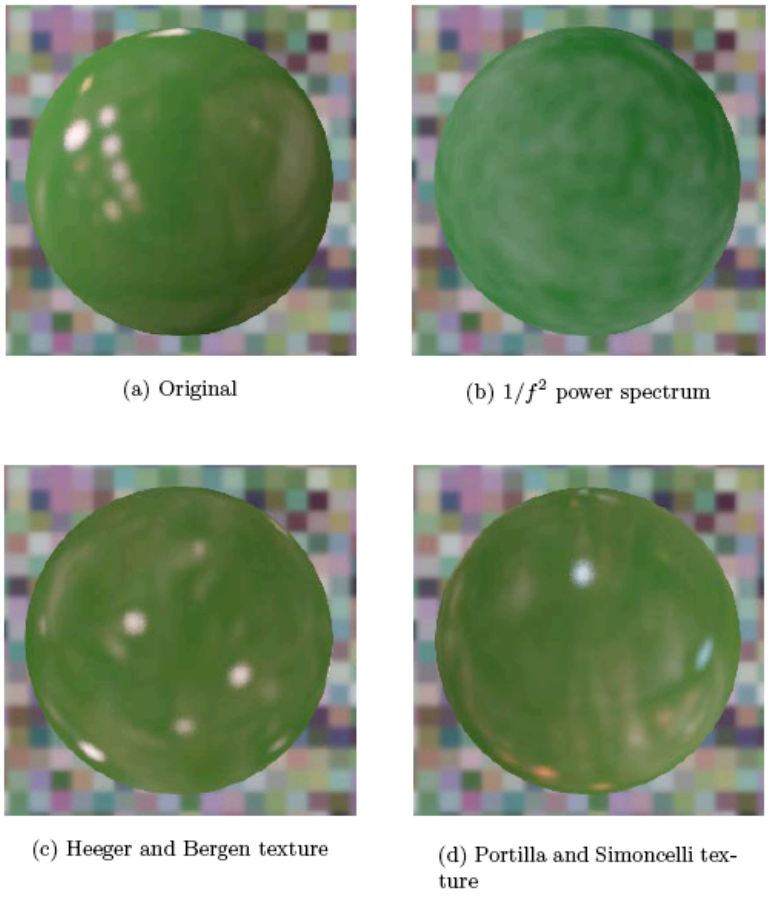

(a) Original

(b) $1/f^2$ power spectrum

(c) Heeger and Bergen texture

(d) Portilla and Simoncelli texture

Figure 4.14. Spheres of identical reflectance properties rendered under a photographically-acquired illumination map (a) and three synthetic illumination maps (b-d). The illumination in (b) is Gaussian noise with a $1/f^2$ power spectrum. The illumination in (c) was synthesized with the procedure of Heeger and Bergen [43] to match the pixel histogram and marginal wavelet histograms of the illumination in (a). The illumination in (d) was synthesized using the technique of Portilla and Simoncelli, which also enforces conditions on the joint wavelet histograms. The illumination map of (a) is due to Debevec [24].

Illumination Maps

(a) (b) (c) (d)

Figure 5.2. (a) A photographically-acquired illumination map, illustrated on the inside of a spherical shell. The illumination map is identical to that of Figure 4.1d. (b-d) Three surfaces of different geometry and reflectance rendered under this illumination map using the methods of Appendix B.

Classification

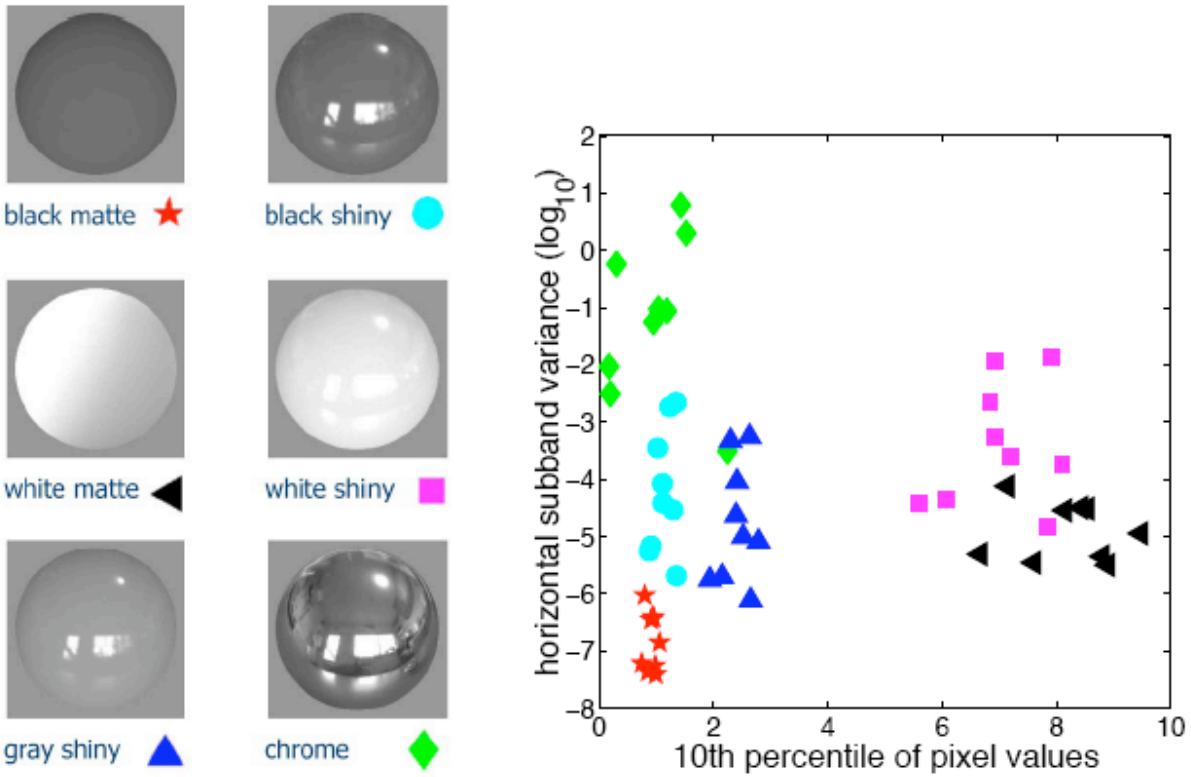

Figure 5.11. At left, synthetic spheres of 6 different reflectances, each rendered under one of Debevec's illumination maps. Ward model parameters are as follows: black matte, $\rho_d = .1$, $\rho_s = 0$; black shiny, $\rho_d = .1$, $\rho_s = .1$, $\alpha = .01$; white matte, $\rho_d = .9$, $\rho_s = 0$; white shiny, $\rho_d = .7$, $\rho_s = .25$, $\alpha = .01$; chrome, $\rho_d = 0$, $\rho_s = .75$, $\alpha = 0$; gray shiny, $\rho_d = .25$, $\rho_s = .05$, $\alpha = .01$. We rendered each sphere under the nine photographically-acquired illuminations depicted in Figure 2.7 and plotted a symbol corresponding to each in the two-dimensional feature space at right. The horizontal axis represents the 10th percentile of pixel intensity, while the vertical axis is the log variance of horizontally-oriented QMF wavelet coefficients at the second-finest scale, computed after geometrically distorting the original image as described in Section 6.1.2.

Classification Continued

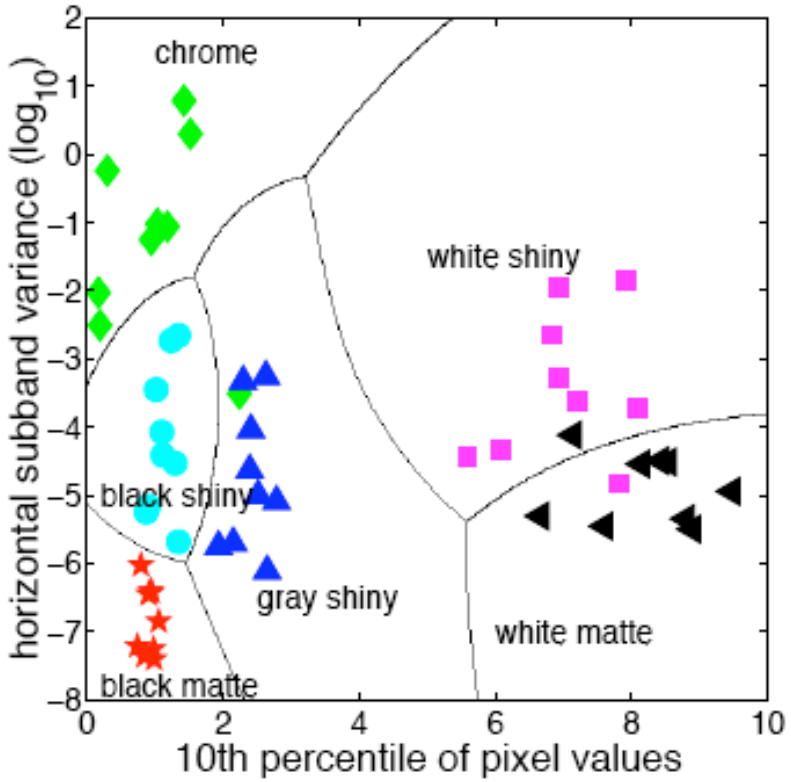

Figure 5.12. The curved lines separate regions assigned to different reflectances by a simple classifier based on two image features. The training examples are the images described in Figure 5.11. The classifier is a one-versus-all support vector machine, described in Section 6.1.1. Using additional image features improves classifier performance.

Photometry

- Photometry:

  Concerned with mechanisms for converting light energy into electrical energy.

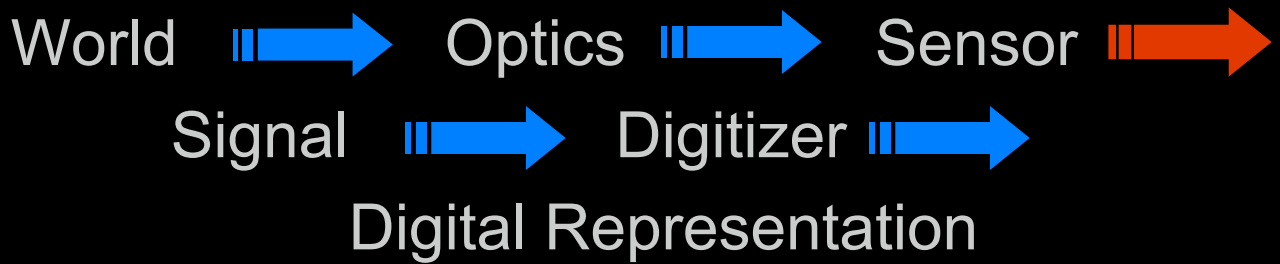

B&W Video System

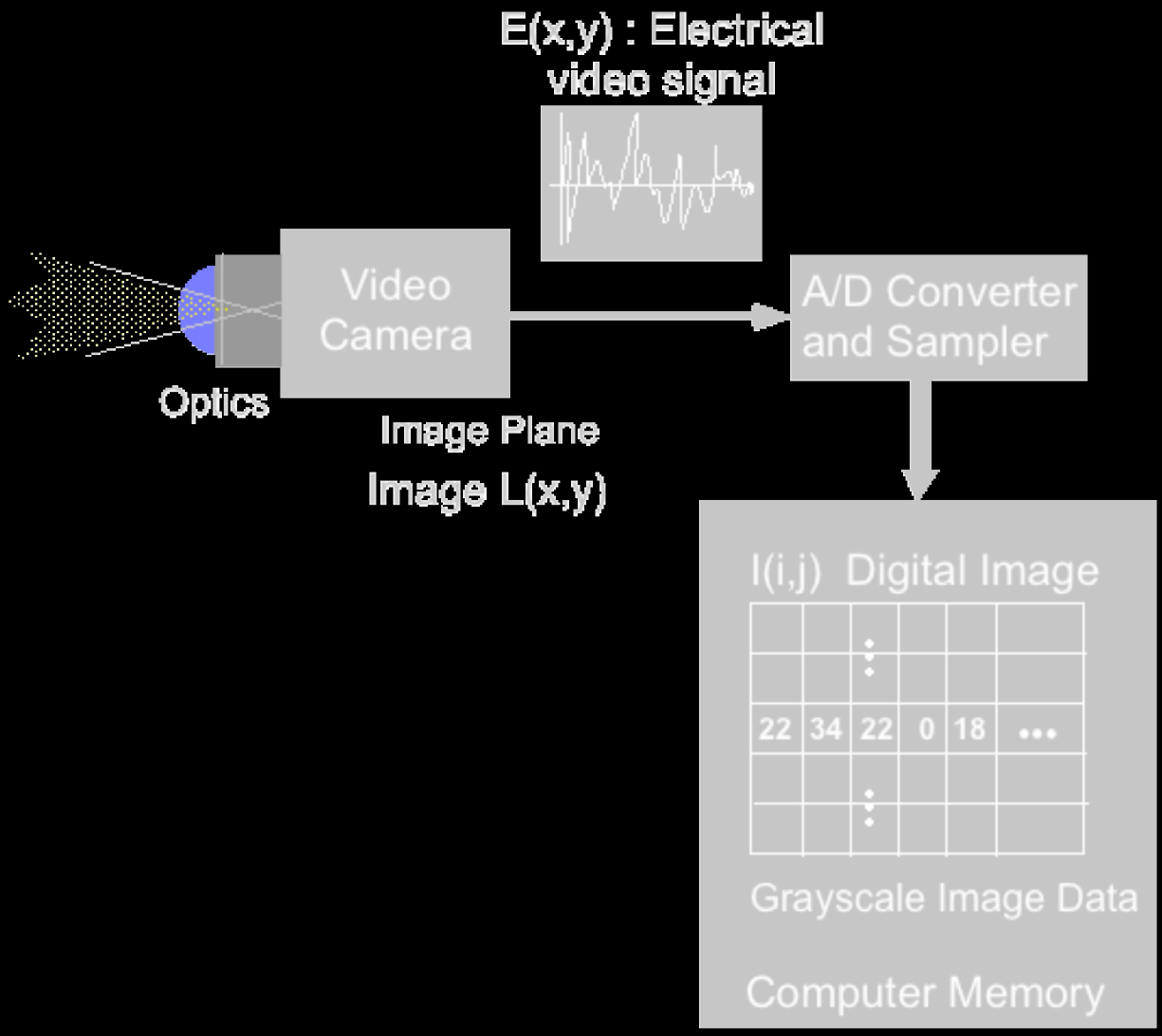

Color Video System

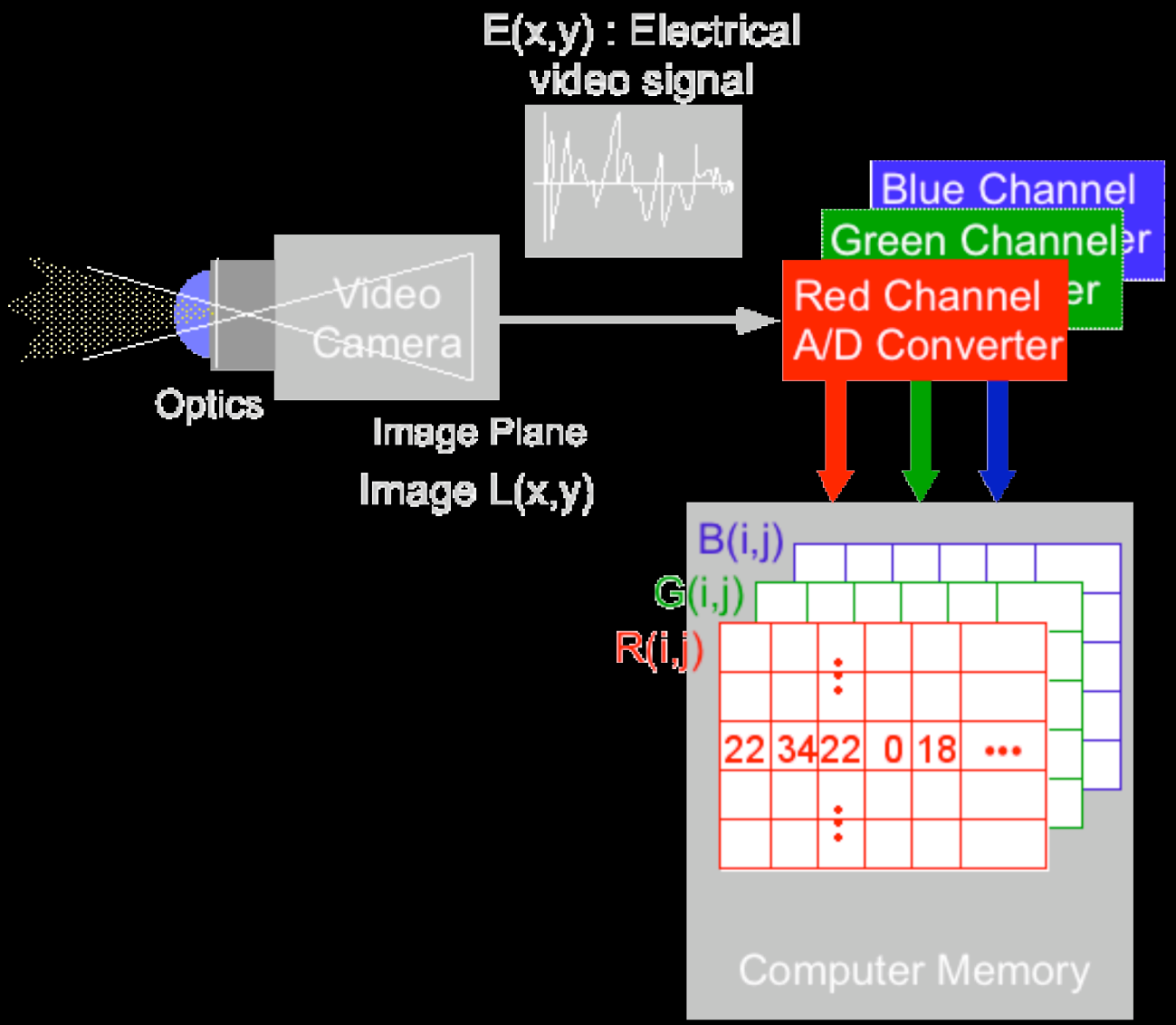

Spectral Sensitivity

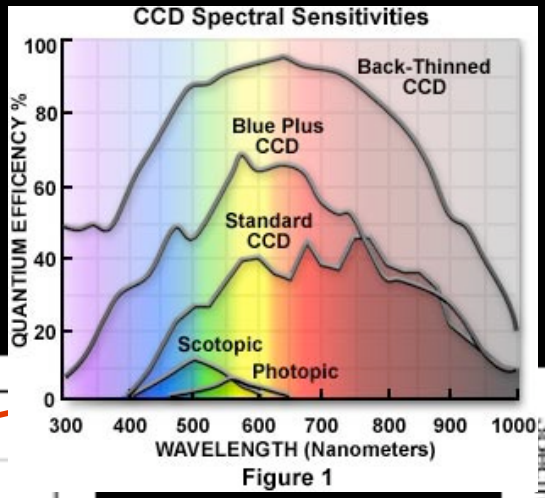

Figure 1

Human Eye

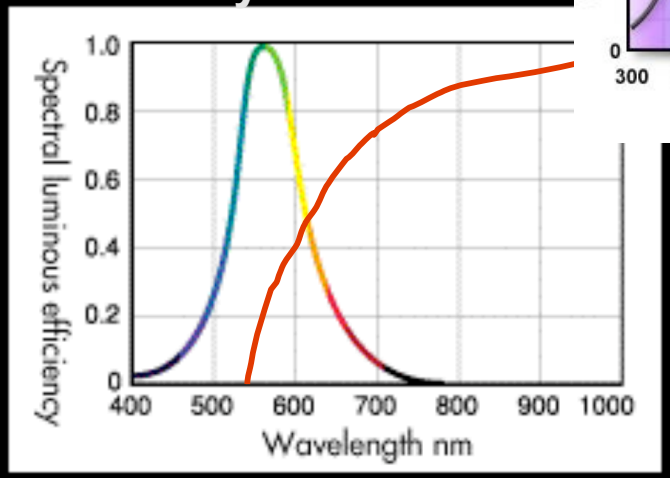

CCD Camera

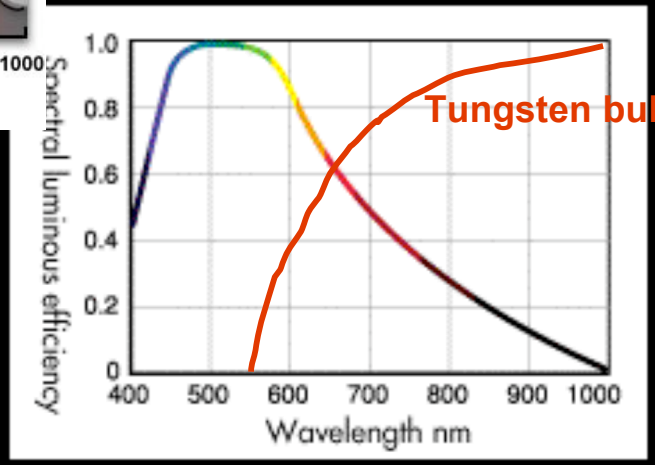

- Figure 1 shows relative efficiency of conversion for the eye (scotopic and photopic curves) and several types of CCD cameras. Note the CCD cameras are much more sensitive than the eye.
- Note the enhanced sensitivity of the CCD in the Infrared and Ultraviolet (bottom two figures)
- Both figures also show a handrawn sketch of the spectrum of a tungsten light bulb

Characteristics

- In general, $V(x,y) = k\, E(x,y)^{\gamma}$ where
  - k is a constant
  - **γ is a parameter of the type of sensor**
    - **γ=1 (approximately) for a CCD camera**
    - **γ=.65 for an old type vidicon camera**
- Factors influencing performance:
  - Optical distortion: pincushion, barrel, non-linearities
  - Sensor dynamic range (30:1 CCD, 200:1 vidicon)
  - Sensor Shading (nonuniform responses from different locations)
- **TV Camera pros: cheap, portable, small size**
- **TV Camera cons: poor signal to noise, limited dynamic range, fixed array size with small image (getting better)**

Sensor Performance

- Optical Distortion: pincushion, barrel, non-linearities
- Sensor Dynamic Range: (30:1 for a CCD, 200:1 Vidicon)
- Sensor Blooming: spot size proportional to input intensity
- Sensor Shading: (non-uniform response at outer edges of image)
- Dead CCD cells

There is no “universal sensor”.
Sensors must be selected/tuned for a particular domain and application.

Lens Aberrations

- In an ideal optical system, all rays of light from a point in the object plane would converge to the same point in the image plane, forming a clear image.
- The lens defects which cause different rays to converge to different points are called aberrations.
  - Distortion: barrel, pincushion
  - Curvature of field
  - Chromatic aberration
  - Spherical aberration
  - Coma
  - Astigmatism

Aberration slides after http://hyperphysics.phy-astr.gsu.edu/hbase/geoopt/aberrcon.html#c1

Lens Aberrations

- Distortion

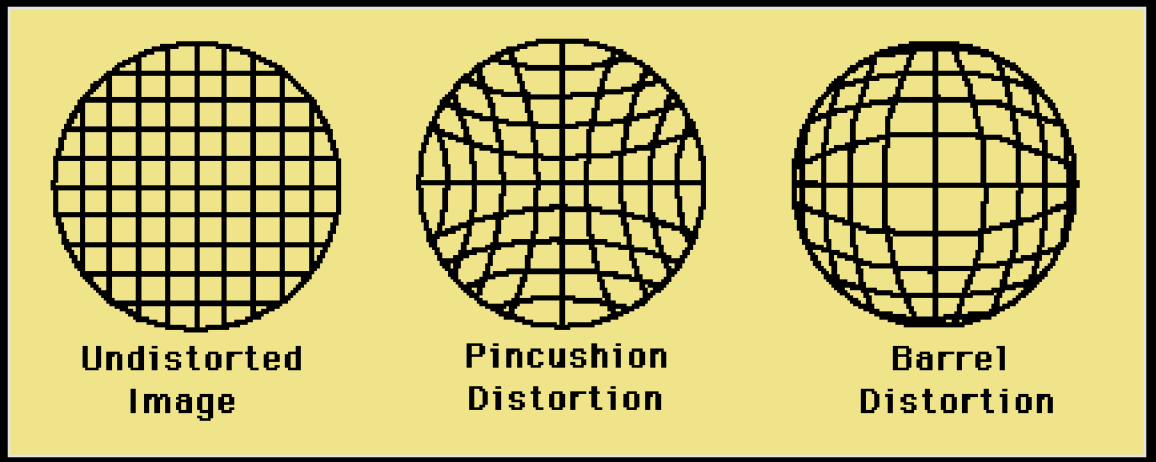

- Curved Field

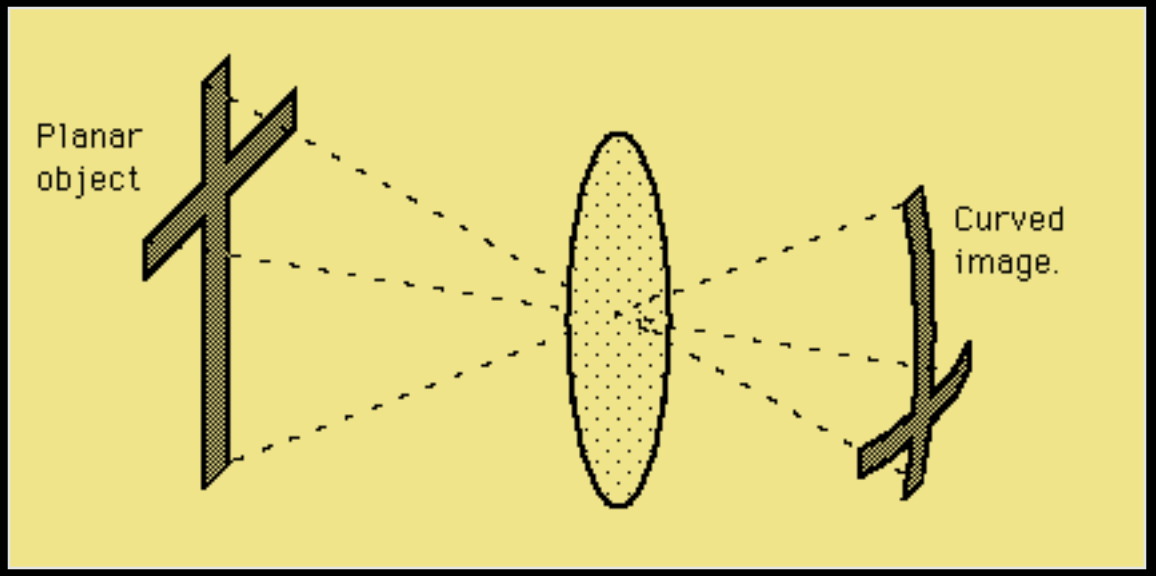

Lens Aberrations

- Chromatic Aberration

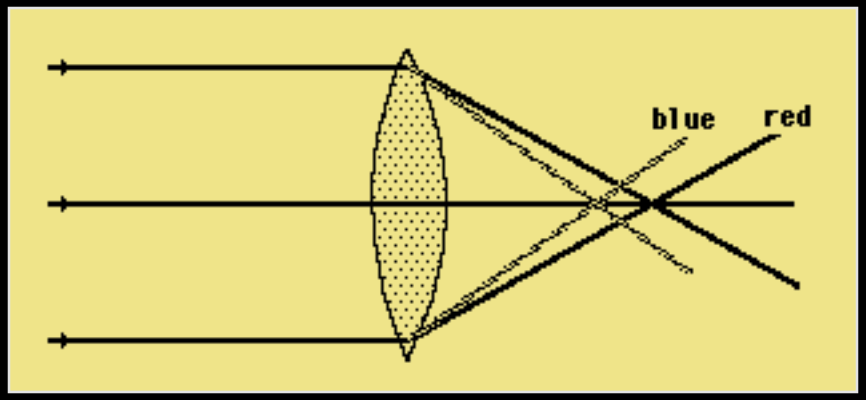

- Focal Length of lens depends on refraction and
- The index of refraction for blue light (short wavelengths) is larger than that of red light (long wavelengths).
- Therefore, a lens will not focus different colors in exactly the same place
- The amount of chromatic aberration depends on the dispersion (change of index of refraction with wavelength) of the glass.

Lens Aberration

- Spherical Aberration

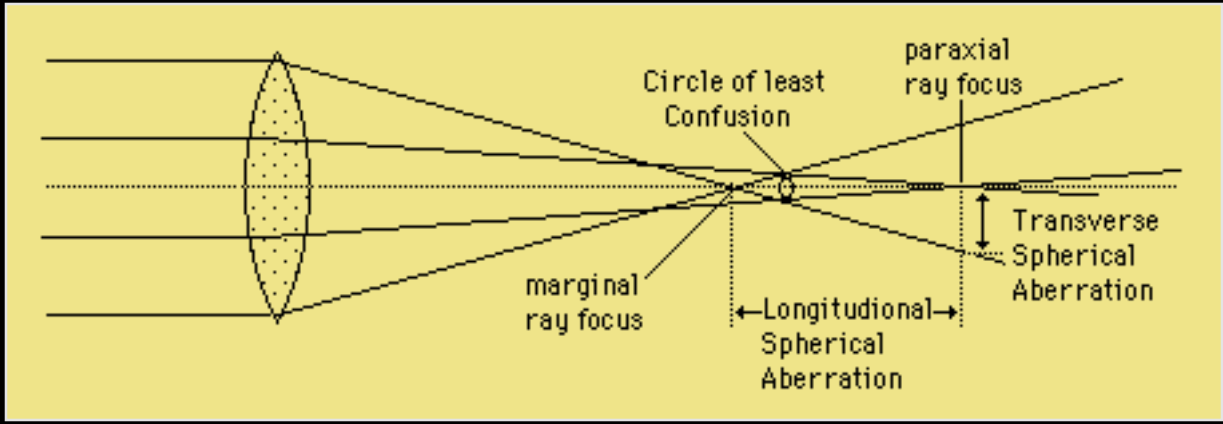

- Rays which are parallel to the optic axis but at different distances from the optic axis fail to converge to the same point.

Lens Aberrations

- Coma

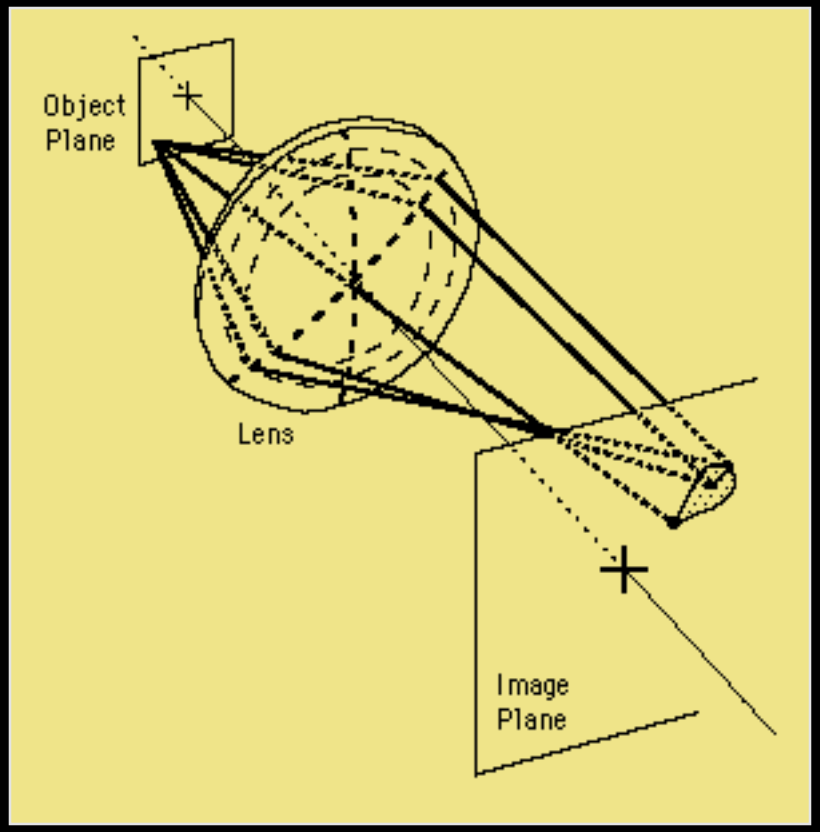

- Rays from an off-axis point of light in the object plane create a trailing "comet-like" blur directed away from the optic axis
- Becomes worse the further away from the central axis the point is

Lens Aberrations

- Astigmatism

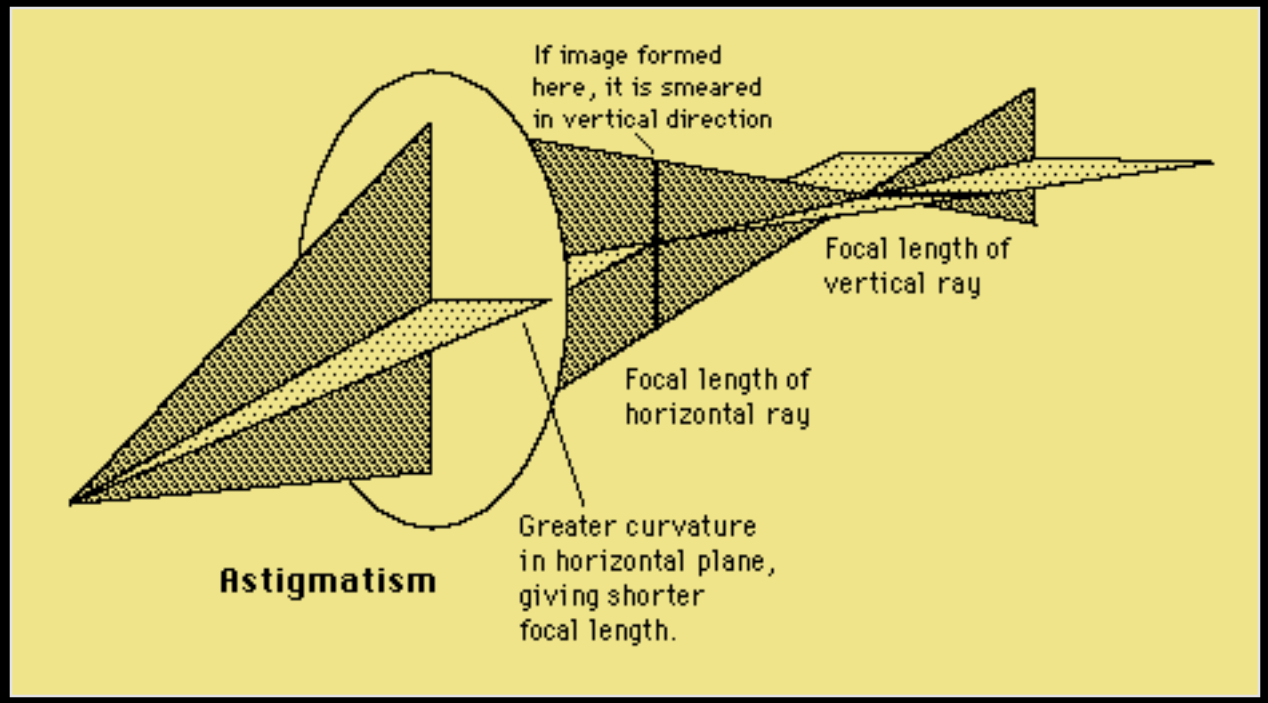

- Results from different lens curvatures in different planes.

Sensor Summary

- Visible Light/Heat
  - Camera/Film combination
  - Digital Camera
  - Video Cameras
  - FLIR (Forward Looking Infrared)
- Range Sensors
  - Radar (active sensing)
    - sonar
    - laser
  - Triangulation
    - stereo
    - structured light
      - – striped, patterned
    - Moire
    - Holographic Interferometry
    - Lens Focus
    - Fresnel Diffraction
- Others
- Almost anything which produces a 2d signal that is related to the scene can be used as a sensor